INCLUSIVE PUBLISHING
TRUSTED SCIENCE

PAPER • OPEN ACCESS

Periodic orbits around the collinear equilibrium points for binary Sirius, Procyon, Luhman 16, *α*-Centuari and Luyten 726-8 systems: the spatial case

View the article online for updates and enhancements.

Journal of Physics Communications

PAPER

Periodic orbits around the collinear equilibrium points for binary Sirius, Procyon, Luhman 16, α-Centuari and Luyten 726-8 systems: the spatial case

Jagadish Singh[1], A E Perdiou[2], Jessica Mrumun Gyegwe[3,5] and V S Kalantonis[4]

[1] Department of Mathematics, Ahmadu Bello University, Zaria, Nigeria
[2] Department of Civil Engineering, University of Patras, GR-26500 Patras, Greece
[3] Department of Mathematical sciences, Federal University Lokoja, Lokoja, Kogi State, Nigeria
[4] Department of Electrical & Computer Engineering, University of Patras, GR-26500 Patras, Greece
[5] Author to whom any correspondence should be addressed

E-mail: jgds2004@yahoo.com, aperdiou@upatras.gr, jessica.gyegwe@fulokoja.edu.ng and kalantonis@upatras.gr
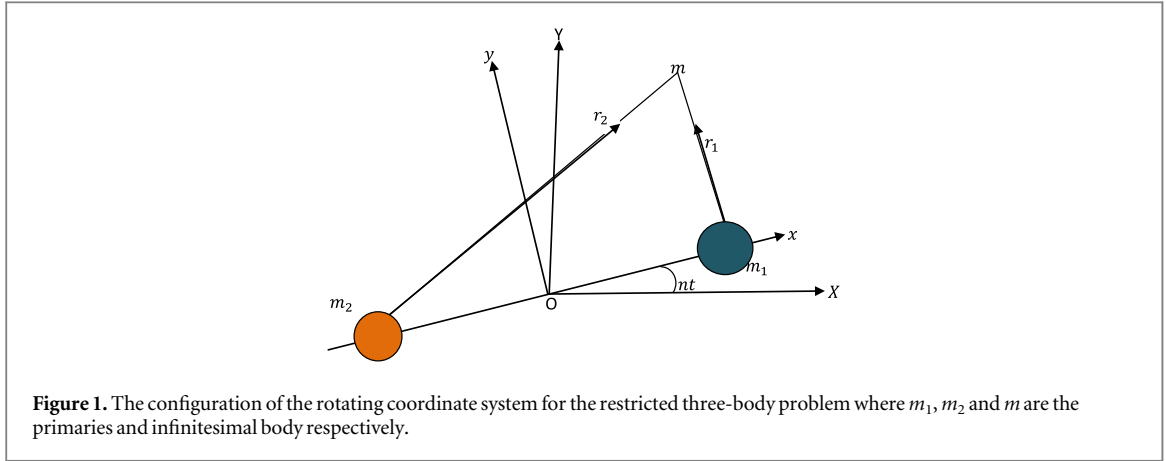
Abstract

An investigation of three-dimensional periodic orbits and their stability emanating from the collinear equilibrium points of the restricted three-body problem with oblate and radiating primaries is presented. A simulation is done by using five binary systems: Sirius, Procyon, Luhman 16, α-Centuari and Luyten 726-8. Firstly, based on the topological degree theory, the total number of the collinear equilibrium points for the five binary systems were obtained and then, their positions were determined numerically. The linear stability of these equilibrium points was also examined and found to be unstable in the Lyapunov sense. An analytical approximation of three-dimensional periodic solutions around them was established via the Lindstedt–Poincaré local analysis. Finally, using the analytical solution to obtain starting orbits, the families of three-dimensional periodic orbits emanating from these equilibria have been continued numerically.

1. Introduction

In the circular planar restricted three-body problem, two point masses or primaries are fixed in a coordinate system rotating at the orbital angular velocity with the origin at the barycentre of the two primaries (as illustrated in figure 1). It is well known that in this rotating frame, there are five stationary points at which the infinitesimal body would remain fixed if placed there. Three of these stationary (or equilibrium) points lie on the line connecting the two primaries and are otherwise known as the collinear equilibrium points denoted as L_1, L_2, L_3, while the other two which form triangular configuration with the primaries in the plane of primaries' motion are called triangular equilibrium points and are denoted by L_4, L_5.

Studies on periodic orbits around these equilibrium points have aided meaningful developments in the fields of celestial mechanics and space explorations. Researchers have utilized different approaches in order to examine periodic orbits around the equilibrium points and in particular, the collinear equilibrium points (Richardson 1980, Howell 1984, Kalantonis *et al* 2001, Lara and Peláez 2002, Hou and Liu 2009, Liu *et al* 2014, Jiang 2015, Zotos 2015, Abouelmagd *et al* 2016). The stability of planar periodic orbits in the vicinity of the collinear equilibrium points either for in-plane or out-of-plane perturbations have been studied by Hénon (1965, 1973), Ragos and Zagouras (1991), Jain *et al* (2006). Recently, Singh *et al* (2016) examined periodic motions around the collinear points of the restricted three-body problem where the primary is a triaxial rigid body and the secondary is an oblate spheroid together with perturbation in the Coriolis and centrifugal forces.

Studies on periodic orbits with applications to the stellar systems are very important in Astrophysics. The masses of the stars in a binary system can be indirectly obtained from the calculation of their orbits. As a result, other stellar parameters like radius and density can be estimated. The masses of single stars can also be estimated by the determination of their empirical mass-luminosity relationship. Nagel and Pichardo (2008) gave a simple

Figure 1. The configuration of the rotating coordinate system for the restricted three-body problem where m_1, m_2 and m are the primaries and infinitesimal body respectively.

analytical formulation for periodic orbits in binary stars. Bosanac *et al* (2015) investigated periodic motions near a large mass ratio binary in the restricted three-body problem where stability analysis was used to evaluate the effect of the mass ratio on the structure of families of periodic orbits. For an investigation on periodic orbits around the triangular points with applications to the binary stellar systems: Kepler-34, Kepler-35, Kepler-413, and Kepler-16, Mia and Kushvah (2016) applied the Fourier series method to obtain them semi-analytically.

In the present work we consider the five binary systems Sirius, Procyon, Luhman 16, α-Centuari and Luyten 726-8 modeled as being radiating sources and sufficiently oblate in the framework of the spatial restricted three-body problem. In our investigation we firstly determine the number and positions of the collinear equilibrium points for all five binary systems and then examine their linear stability. We then apply the Lindstedt–Poincaré method in order to obtain analytical expressions up to second order terms for three-dimensional periodic orbits around the collinear equilibria. The analytical investigation has been also used to obtain starting points in order to compute numerically the families of three-dimensional periodic orbits emanating from these points. The stability of these orbits has also been examined.

2. Equations of motion and variation

The equations of motion of the infinitesimal body in the dimensionless synodic coordinate system *Oxyz* i.e., taking the units of mass, length and time such that the sum of the masses of the primaries, the distance between them and the gravitational constant are all unity, with the bigger and smaller stars of the binary systems having masses m_1 and m_2, with the mass parameter being $\mu = m_2/(m_1 + m_2)$, and radiation pressure and oblateness parameters taken as q_1, q_2 ($q_i \leqslant 1$, $i = 1, 2$) and A_1, A_2 ($A_i \ll 1$, $i = 1, 2$), respectively, are (Singh and Ishwar 1999):

$$\ddot{x} - 2n\dot{y} = \Omega_x,$$
$$\ddot{y} + 2n\dot{x} = \Omega_y,$$
$$\dot{z} = \Omega_z, \tag{1}$$

where the potential function is given by:

$$\Omega = \frac{1}{2}n^2(x^2 + y^2) + \frac{(1-\mu)q_1}{r_1} + \frac{\mu q_2}{r_2} + \frac{(1-\mu)A_1 q_1}{2r_1^3} + \frac{\mu A_2 q_2}{2r_2^3}$$
$$- \frac{3(1-\mu)z^2 A_1 q_1}{2r_1^5} - \frac{3\mu A_2 q_2 z^2}{2r_2^5},$$

the angular velocity:

$$n = \sqrt{1 + \frac{3}{2}(A_1 + A_2)},$$

and

$$r_1 = \sqrt{(x - \mu) + y^2 + z^2}, \quad r_2 = \sqrt{(x - \mu + 1) + y^2 + z^2},$$

are the distances of the infinitesimal mass body from the two stars, respectively.

In the six-dimensional phase space, equation (1) can be written in the form:

$$\dot{x}_i = f_i(x_1, x_2, \ldots, x_6), \quad i = 1, 2, \ldots, 6,$$

with

$$f_1 = x_4, \quad f_2 = x_5, \quad f_3 = x_6,$$

$$f_4 = 2nx_5 + n^2 x_1 + \frac{15A_1(1-\mu)q_1(x_1-\mu)x_3^2}{2r_{10}^7} - \frac{3A_1(1-\mu)q_1(x_1-\mu)}{2r_{10}^5} - \frac{(1-\mu)q_1(x_1-\mu)}{r_{10}^3}$$

$$+ \frac{15A_2\mu q_2(x_1+1-\mu)x_3^2}{2r_{20}^7} - \frac{3A_2\mu q_2(x_1+1-\mu)}{2r_{20}^5} - \frac{\mu q_2(x_1+1-\mu)}{r_{10}^3},$$

$$f_5 = -2nx_4 + n^2 x_2 + \frac{15A_1(1-\mu)q_1 x_2 x_3^2}{2r_{10}^7} - \frac{3A_1(1-\mu)q_1 x_2}{2r_{10}^5} - \frac{(1-\mu)q_1 x_2}{r_{10}^3} + \frac{15A_2\mu q_2 x_2 x_3^2}{2r_{20}^7}$$

$$- \frac{3A_2\mu q_2 x_2}{2r_{20}^5} - \frac{\mu q_2 x_2}{r_{20}^3},$$

$$f_6 = \frac{15A_1(1-\mu)q_1 x_3^3}{2r_{10}^7} - \frac{9A_1(1-\mu)q_1 x_3}{2r_{10}^5} - \frac{(1-\mu)q_1 x_3}{r_{10}^3} + \frac{15A_2\mu q_2 x_3^3}{2r_{20}^7} - \frac{9A_2\mu q_2 x_3}{2r_{20}^5} - \frac{\mu q_2 x_3}{r_{20}^3}, \quad (2)$$

where we have set:

$$x_1 = x, \ x_2 = y, \ x_3 = z, \ x_4 = \dot{x}, \ x_5 = \dot{y}, \ x_6 = \dot{z},$$

while the distances are now expressed by:

$$r_{10} = [(x_1-\mu)^2 + x_2^2 + x_3^2]^{\frac{1}{2}}, \quad r_{20} = [(x_1+1-\mu)^2 + x_2^2 + x_3^2]^{\frac{1}{2}}.$$

The Jacobi integral w.r.t. the equations of motion (2) is given by:

$$C = n^2(x_1^2 + x_2^2) - \frac{3A_1(1-\mu)q_1 x_3^2}{r_{10}^5} + \frac{A_1(1-\mu)q_1}{r_{10}^3} + \frac{2(1-\mu)q_1}{r_{10}} - \frac{3A_2\mu q_2 x_3^2}{r_{20}^5}$$

$$+ \frac{A_2\mu q_2}{r_{20}^3} + \frac{2\mu q_2}{r_{20}} - (x_4^2 + x_5^2 + x_6^2). \quad (3)$$

The coordinates of the third body in the six-dimensional phase space depend uniquely along any solution on the initial conditions and the time, i.e.:

$$x_i = x_i(x_{01}, x_{02}, \ldots, x_{06}; t), \quad i = 1, 2, \ldots, 6,$$

and their partial derivatives with respect to the initial conditions satisfy the equations of variation (see, e.g., Zagouras and Markellos 1977, Jain *et al* 2006):

$$\frac{d}{dt}\left(\frac{\partial x_i}{\partial x_{0j}}\right) = \sum_{k=1}^{6} \frac{\partial f_i}{\partial x_k}\frac{\partial x_k}{\partial x_{0j}}, \quad i, j = 1, 2, \ldots, 6.$$

The variational equations can be written as follows:

$$\dot{v}_{ij} = v_{(i+3)j}, \quad i = 1, 2, 3, \quad j = 1, 2, \ldots, 6,$$

$$\dot{v}_{ij} = f_{i1}v_{1j} + f_{i2}v_{2j} + f_{i3}v_{3j} + f_{i4}v_{4j} + f_{i5}v_{5j}, \quad i = 4, 5, 6, \quad j = 1, 2, \ldots, 6, \quad (4)$$

where we have denoted $v_{ij} = \partial x_i/\partial x_{0j}$ and $f_{ij} = \partial f_i/\partial x_{0j}$ with:

$$f_{41} = n^2 - \frac{105A_1(1-\mu)q_1(x_1-\mu)^2 x_3^2}{2r_1^9} + \frac{15A_1(1-\mu)q_1(x_1-\mu)^2}{2r_1^7}$$

$$+ \frac{15A_1(1-\mu)q_1 x_3^2}{2r_1^7} - \frac{3A_1(1-\mu)q_1}{2r_1^7} + \frac{3(1-\mu)q_1(x_1-\mu)^2}{r_1^5}$$

$$- \frac{(1-\mu)q_1}{r_1^3} - \frac{105A_2\mu q_2(x_1+1-\mu)^2 x_3^2}{2r_2^9} - \frac{15A_2\mu q_2(x_1+1-\mu)^2}{2r_2^7}$$

$$+ \frac{15A_2\mu q_2 x_3^2}{2r_2^7} - \frac{3A_2\mu q_2}{2r_2^5} + \frac{3\mu(x_1+1-\mu)^2}{r_2^5} - \frac{\mu q_2}{r_2^3},$$

Table 1. Physical parameters of the five binary systems.

Parameters	Sirius	Procyon	Luhman 16	α-Centuari	Luyten 726-8
M_A	$1.99 M_s$	$1.57 M_s$	$63 M_J$	$1.14 M_S$	$0.11 M_S$
M_B	$0.98 M_s$	$0.88 M_s$	$49 M_J$	$0.92 M_S$	$0.1 M_S$
μ	0.3300	0.3592	0.4375	0.4466	0.4762
$L_A(L_S)$	22.5	7.59	1.7×10^{-9}	1.54	5.65×10^{-5}
$L_B(L_S)$	2.54×10^{-3}	5.6×10^{-4}	0.8×10^{-9}	0.453	3.7×10^{-5}
q_1	0.976 734	0.990 052	1	0.997 220	0.999 999
q_2	0.999 995	0.999 999	1	0.996 555	0.999 999
A_1	0.10	0.12	0.14	0.16	0.17
A_2	0.11	0.13	0.15	0.18	0.19

$$f_{42} = -\frac{105 A_1 (1-\mu) q_1 (x_1 - \mu) x_2 x_3^2}{2 r_1^9} + \frac{15 A_1 (1-\mu) q_1 (x_1 - \mu) x_2}{2 r_1^7}$$
$$+ \frac{3(1-\mu) q_1 (x_1 - \mu) x_2}{r_1^5} - \frac{105 A_2 \mu q_2 (x_1 - \mu) x_2 x_3^2}{2 r_2^9}$$
$$+ \frac{15 A_2 \mu q_2 (x_1 + 1 - \mu) x_2}{2 r_2^7} + \frac{3 \mu q_2 (x_1 + 1 - \mu) x_2}{r_2^5},$$

$$f_{43} = -\frac{105 A_1 (1-\mu) q_1 (x_1 - \mu) x_3^3}{2 r_1^9} + \frac{45 A_1 (1-\mu) q_1 (x_1 - \mu) x_3}{2 r_1^7}$$
$$+ \frac{3(1-\mu) q_1 (x_1 - \mu) x_3}{r_1^5} - \frac{105 A_2 \mu q_2 (x_1 + 1 - \mu) x_3^3}{2 r_2^9}$$
$$+ \frac{45 A_2 \mu q_2 (x_1 + 1 - \mu) x_3}{2 r_2^7} + \frac{3 \mu q_2 (x_1 + 1 - \mu) x_3}{r_2^5},$$

$$f_{44} = 0, \quad f_{45} = 2n, \quad f_{51} = f_{42},$$
$$f_{52} = n^2 - \frac{105 A_1 (1-\mu) q_1 x_2^3 x_3^3}{2 r_1^9} + \frac{15 A_1 (1-\mu) q_1 x_2^2}{2 r_1^2} + \frac{105 A_1 (1-\mu) q_1 x_3^2}{2 r_1^7}$$
$$- \frac{3 A_1 (1-\mu) q_1}{2 r_1^5} + \frac{3(1-\mu) q_1 x_2^2}{2 r_1^5} - \frac{(1-\mu) q_1}{r_1^3} - \frac{105 A_2 \mu q_2 x_2^2 x_3^2}{2 r_2^9}$$
$$+ \frac{15 A_2 \mu q_2 x_2^2}{2 r_1^7} + \frac{15 A_2 \mu q_2 x_3^2}{2 r_2^7} - \frac{3 A_2 \mu q_2}{2 r_2^5} + \frac{3 \mu q_2 x_2^2}{r_2^5} - \frac{\mu q_2}{r_2^3},$$

$$f_{53} = -\frac{105 A_1 (1-\mu) q_1 x_2 x_3^3}{2 r_1^9} + \frac{45 A_1 (1-\mu) q_1 x_2 x_3}{2 r_1^7} + \frac{3(1-\mu) q_1 x_2 x_3}{r_1^5} - \frac{105 A_2 \mu q_2 x_2 x_3^3}{2 r_2^9}$$
$$+ \frac{45 A_2 \mu q_2 x_2 x_3}{2 r_2^7} + \frac{3 \mu q_2 x_2 x_3}{r_2^5},$$

$$f_{54} = -2n, \quad f_{55} = 0, \quad f_{61} = f_{43}, \quad f_{62} = f_{53},$$

$$f_{63} = -\frac{105 A_1 (1-\mu) q_1 x_3^4}{2 r_1^9} + \frac{45 A_1 (1-\mu) q_1 x_3^2}{r_1^7} - \frac{9 A_1 (1-\mu) q_1}{2 r_1^5} + \frac{3(1-\mu) q_1 x_3^2}{r_1^5}$$
$$- \frac{(1-\mu) q_1}{r_1^3} - \frac{105 A_2 \mu q_2 x_3^4}{2 r_2^9} + \frac{45 A_2 \mu q_2 x_3^2}{2 r_2^7} - \frac{9 A_2 \mu q_2}{2 r_2^5} + \frac{3 \mu q_2 x_3^2}{r_2^5} - \frac{\mu q_2}{r_2^3},$$

$$f_{64} = 0, \quad f_{65} = 0. \tag{5}$$

3. Numerical values of the physical parameters

In table 1, we present the physical parameters of the binary systems. The parameters M_A and M_B are the masses of the more massive and less massive stars in each binary system as compared to the mass of the Sun, with an exception of the binary Luhman 16 system where comparison is being to the mass of Jupiter. The luminosity of the binary systems denoted by L_A and L_B respectively is obtained from the relation (Mia and Kushvah 2016):

Table 2. The collinear equilibrium points for the five binary systems.

Binary systems	L_1	L_2	L_3
Sirius	−1.261 856 48	−0.219 703 40	1.108 341 59
Procyon	−1.252 405 46	−0.181 002 28	1.123 258 96
Luhman 16	−1.221 055 85	−0.078 606 60	1.160 729 79
α-Centuari	−1.218 094 49	−0.064 316 50	1.161 264 75
Luyten 726-8	−1.205 334 06	−0.026 095 29	1.175 571 31

$$\frac{L}{L_S} \approx \left(\frac{M}{M_S}\right)^{3.9},$$

where L_S and M_S are the luminosity and mass of the Sun.

Radiation pressure has had a key effect on the formation of stars and shaping of clouds of dust and gases on a wide range of scales. The mass reduction factor is represented as $q_i = 1 - F_p/F_g$, $i = 1$, 2 (F_p and F_g are the radiation pressure and the gravitational attraction forces being exerted by the binary systems on objects around them) or $q_i = 1 - \beta$, $i = 1$, 2 or on the basis of the Stefan–Boltzmann's law (Xuetang and Lizhong 1993) as:

$$q_i = 1 - \frac{A\kappa L}{a\rho M}, \quad i = 1, \ 2,$$

where M, L, and κ are the mass, luminosity, and radiation pressure efficiency factor of a star. Also, a and ρ are the radius and density of the dust grain particles moving in the binary systems while $A = \frac{3}{16\pi cG}$ is a constant with c and G as the speed of light and the gravitational constant, respectively. The values of the luminosity and mass reduction factor q_i, $i = 1$, 2 have been obtained by computing in the *C.G.S.* system of unit, using $L_s = 3.846 \times 10^{33}$ erg s^{-1}, $c = 3 \times 10^{10}$ cm s^{-1}, $G = 6.673\ 84 \times 10^{-8}$ cm^3 g^{-1}s^{-2}, $M_s = 1.989 \times 10^{33}$ g, $M_J = 1.898 \times 10^{30}$ g and $\kappa = 1$. Also, we have assumed the values for the radius and density of the dust grain particles as $a = 2 \times 10^{-2}$ cm and $\rho = 1.4$ g cm^{-3} (Xuetang and Lizhong 1993, Singh and Umar 2013). Arbitrary values are been used for the oblateness coefficients A_1 and A_2 as shown in table 1.

4. Determination of the collinear equilibrium points and stability

4.1. Locations of the collinear equilibrium points

The collinear equilibrium points lie on the *x*-axis together with the primary bodies. There are three intervals on this line: $(-\infty, \ -1 + \mu)$, $(-1 + \mu, \ \mu)$ and $(\mu, \ +\infty)$, as these are formed by the positions of the two stars. These equilibria are the solutions of the nonlinear algebraic equation arising from (2) for $x_2 = x_3 = 0$ and zero velocity and accelerator components:
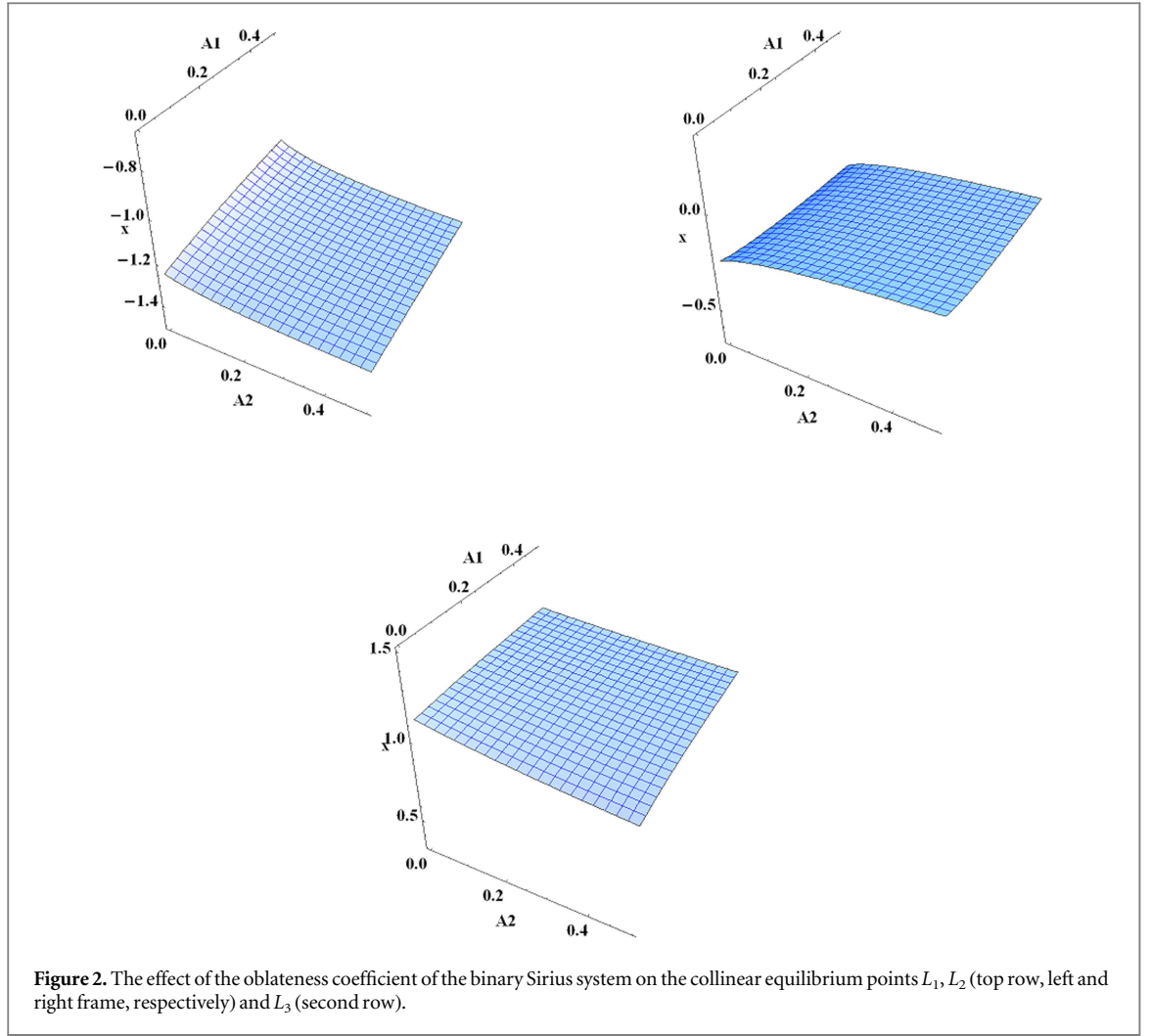
$$f_4(x_1) = 0. \tag{6}$$

The determination of the exact number of roots of equation (6), at each one of the above mentioned open intervals, has been established by an approach based on the topological degree theory and can be briefly described as follows: if the function $F(x)$: $x \in [a, \ b] \subset \mathbb{R}$ is two times continuously differentiable in this interval, then the total number N of roots of the equation $F(x) = 0$ is obtained by the following scheme (Picard 1892, Kalantonis *et al* 2001, Singh and Begha 2011):

$$N = \frac{-\gamma}{\pi} \int_a^b \frac{F(x)F''(x) - F'^2(x)}{F^2(x) + \gamma^2 F'^2(x)} dx + \frac{1}{\pi} \arctan\left(\frac{\gamma \ F(a)F'(b) - F(b)F'(a)}{F(a)F(b) + \gamma^2 \ F'(a)F'(b)}\right),$$

where γ is a small positive real constant. For all the considered binary systems, i.e. for the parameter values corresponding to the specific systems, we have shown that each one of the aforementioned open intervals contains a unique real root; these roots correspond to the collinear equilibrium points L_1, L_2 and L_3, respectively. Note, that the involved integral in the above formula has been computed numerically by using Romberg integration. Since we have determined the exact number of the collinear equilibrium points we are able to solve numerically (6) so as to obtain their positions accurately. These are shown in table 2 for each binary system. Also, in figure 2 we present the effect of the oblateness coefficients on the positions of all collinear equilibrium points of the Sirius binary system while in figure 3 we show the effect of radiation factors on these points of the same system.

4.2. Stability of the collinear equilibrium points

We examine the linear stability of the collinear equilibrium points in the plane of motion of the primaries for each one of the five binary systems by solving numerically the following characteristic equation:

Figure 2. The effect of the oblateness coefficient of the binary Sirius system on the collinear equilibrium points L_1, L_2 (top row, left and right frame, respectively) and L_3 (second row).

$$\omega^4 + (\mathscr{P}_1 + \mathscr{Q}_1 - 4n^2)\omega^2 + \mathscr{P}_1\mathscr{Q}_1 = 0, \tag{7}$$

arising from the linearization of the equations of motion around these equilibria. The coefficients $\mathscr{P}_1$ and $\mathscr{Q}_1$ in the above equation are given in the next section. The roots of equation (7) are presented in table 3 for each one of the five binary systems. As we can see from this table, for all systems and at each collinear equilibrium point four roots exist two of which are real and two pure imaginary. Therefore, the collinear equilibrium points are unstable in the Lyapunov sense. However, by eliminating the hyperbolic component of the general solution of the linearized system around the collinear equilibria, we are able to obtain analytical approximations of periodic motions around these points.

5. Three-dimensional periodic motion around the collinear equilibrium point

In order to study the motion of the infinitesimal body near any of the collinear equilibrium points $L_i, i = 1, 2, 3$, we write

$$x_1 = x_{L_i} + \mathfrak{I}, \; x_2 = \mathfrak{R}, \; \text{and} \; x_3 = \aleph,$$

where $\mathfrak{I}$, $\mathfrak{R}$ and $\aleph$ are small displacements in $(x_{L_i}, 0, 0)$ and are also new coordinates $(L_{\mathfrak{I}}, L_{\mathfrak{R}}$ and $L_{\aleph})$ parallel to Ox, Oy and Oz. By substituting the last equations into equation (2), the equations of motion become

$$\ddot{\mathfrak{I}} - 2n\dot{\mathfrak{R}} = \Omega_{\mathfrak{I}},$$
$$\ddot{\mathfrak{R}} + 2n\dot{\mathfrak{I}} = \Omega_{\mathfrak{R}},$$
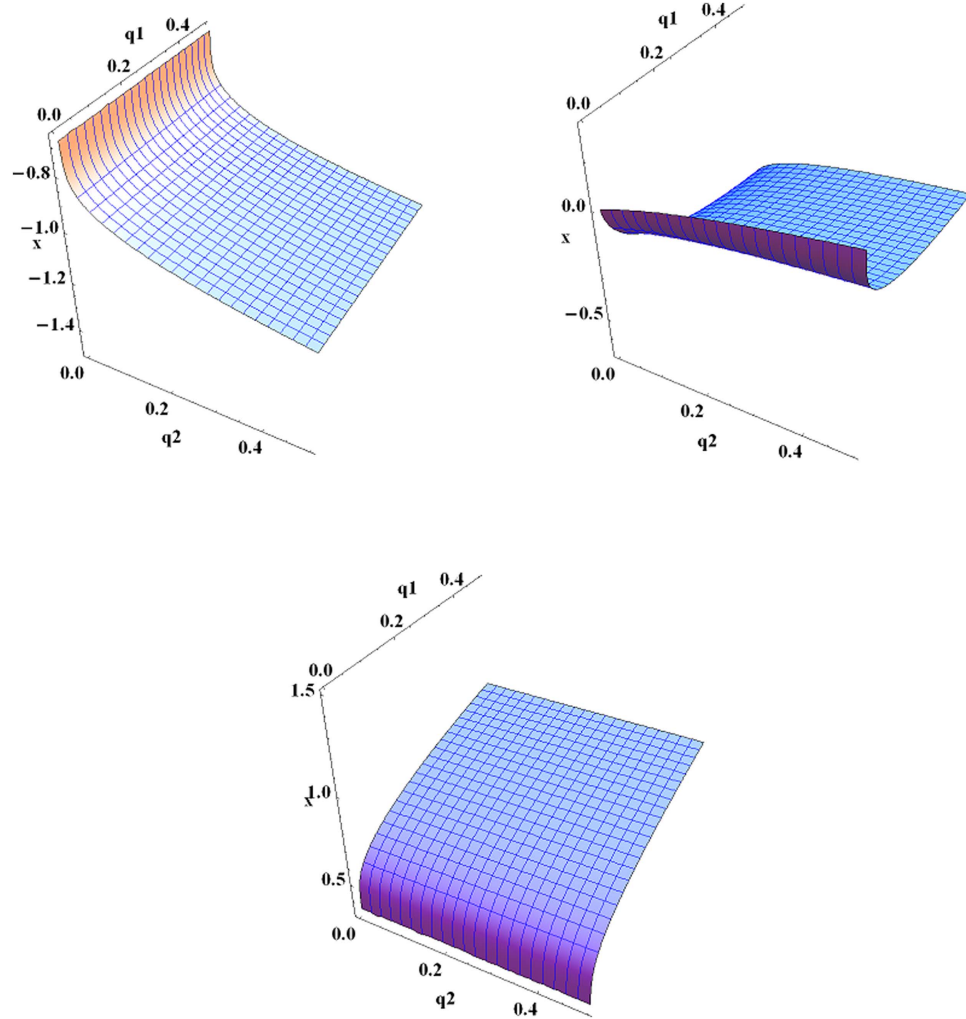$$\ddot{\aleph} \qquad\quad = \Omega_{\aleph}. \tag{8}$$

Figure 3. The effect of the radiation coefficient of the binary Sirius system on the collinear equilibrium points L_1, L_2 (top row, left and right frame, respectively) and L_3 (second row).

Table 3. The roots of the characteristic equation (6) for the five binary systems.

Binary systems	Characteristic roots (L_1)	Characteristic roots (L_2)	Characteristic roots (L_3)
Sirius	$\pm 1.961\ 898\ 49$	$\pm 5.666\ 082\ 02$	$\pm 1.251\ 224\ 83$
	$\pm 1.564\ 308\ 88i$	$\pm 3.534\ 163\ 12i$	$\pm 1.307\ 275\ 49i$
Procyon	$\pm 1.976\ 502\ 49$	$\pm 6.022\ 009\ 57$	$\pm 1.370\ 031\ 42$
	$\pm 1.564\ 586\ 39i$	$\pm 3.690\ 917\ 65i$	$\pm 1.345\ 836\ 37i$
Luhman 16	$\pm 1.875\ 187\ 18$	$\pm 6.385\ 128\ 61$	$\pm 1.595\ 968\ 99$
	$\pm 1.522\ 805\ 57i$	$\pm 3.857\ 247\ 98i$	$\pm 1.426\ 290\ 20i$
α-*Centuari*	$\pm 1.950\ 396\ 23$	$\pm 6.724\ 382\ 75$	$\pm 1.694\ 629\ 82$
	$\pm 1.542\ 545\ 70i$	$\pm 3.999\ 951\ 19i$	$\pm 1.461\ 483\ 19i$
Luyten 726-8	$\pm 1.915\ 163\ 94$	$\pm 6.880\ 781\ 73$	$\pm 1.792\ 158\ 02$
	$\pm 1.527\ 954\ 86i$	$\pm 4.070\ 019\ 89i$	$\pm 1.496\ 640\ 66i$

5.1. Analytical approximation of periodic solutions

Expanding equation (8) into Taylor series up to second order terms we obtain the following system:

$$\ddot{\mathfrak{J}} - 2n\dot{\mathfrak{R}} = \mathscr{P}_1\mathfrak{J} + \mathscr{P}_2\mathfrak{J}^2 + \mathscr{P}_3\mathfrak{R}^2 + \mathscr{P}_4\aleph^2,$$
$$\ddot{\mathfrak{R}} + 2n\dot{\mathfrak{J}} = \mathscr{Q}_1\mathfrak{R} + \mathscr{Q}_2\mathfrak{J}\mathfrak{R},$$
$$\ddot{\aleph} = \mathcal{R}_1\aleph + \mathcal{R}_2\mathfrak{J}\aleph,$$

(9)

where

$$\mathscr{P}_1 = n^2 + 2(1-\mu)q_1\left[\frac{3A_1}{r_{10}^5} + \frac{1}{r_{10}^3}\right] + 2\mu q_2\left[\frac{3A_2}{r_{20}^5} + \frac{1}{r_{20}^3}\right],$$

$$\mathscr{P}_2 = 3(1-\mu)q_1\left[\frac{5A_1}{r_{10}^6} + \frac{1}{r_{10}^4}\right]\vartheta_1 + 3\mu q_2\left[\frac{5A_2}{r_{20}^6} + \frac{1}{r_{20}^4}\right]\vartheta_2,$$

$$\mathscr{P}_3 = -\frac{3(1-\mu)q_1}{2}\left[\frac{5A_1}{2r_{10}^6} + \frac{1}{r_{10}^4}\right]\vartheta_1 - \frac{3\mu q_2}{2}\left[\frac{5A_2}{2r_{20}^6} + \frac{1}{r_{20}^4}\right]\vartheta_2,$$

$$\mathscr{P}_4 = -\frac{3(1-\mu)q_1}{2}\left[\frac{15A_1}{2r_{10}^6} + \frac{1}{r_{10}^4}\right]\vartheta_1 - \frac{3\mu q_2}{2}\left[\frac{15A_2}{2r_{20}^6} + \frac{1}{r_{20}^4}\right]\vartheta_2,$$

$$\mathscr{Q}_1 = n^2 - (1-\mu)q_1\left[\frac{3A_1}{2r_{10}^5} + \frac{1}{r_{10}^3}\right] - \mu q_2\left[\frac{3A_2}{2r_{20}^5} + \frac{1}{r_{20}^3}\right],$$

$$\mathscr{Q}_2 = -3(1-\mu)q_1\left[\frac{15A_1}{2r_{10}^6} + \frac{1}{r_{10}^4}\right]\vartheta_1 - 3\mu q_2\left[\frac{15A_2}{2r_{20}^6} + \frac{1}{r_{20}^4}\right]\vartheta_2,$$

$$\mathcal{R}_1 = -(1-\mu)q_1\left[\frac{9A_1}{2r_{10}^5} + \frac{1}{r_{10}^3}\right] - \mu q_2\left[\frac{9A_2}{2r_{20}^5} + \frac{1}{r_{20}^3}\right],$$

$$\mathcal{R}_2 = -3(1-\mu)q_1\left[\frac{15A_1}{2r_{10}^6} + \frac{1}{r_{10}^4}\right]\vartheta_1 - 3\mu q_2\left[\frac{15A_2}{2r_{20}^6} + \frac{1}{r_{20}^4}\right]\vartheta_2.$$

The symbols ϑ_1 and ϑ_2 represent the signs of $r_{10} = |x_1 - \mu|$ and $r_{20} = |x_1 + 1 - \mu|$ at any equilibrium point avoiding thus the absolute values for each case. Using the method of successive approximations for solving system (9) we look for periodic solutions of the form:

$$\mathcal{I} = \mathcal{I}_{12}\varepsilon^2, \quad \mathfrak{R} = \mathfrak{R}_{22}\varepsilon^2, \quad \aleph = \aleph_{31}\varepsilon,$$

where ε is a small orbital parameter. Using them in system (9) we find that:

$$\ddot{\mathcal{I}}_{12}'' - 2n\dot{\mathfrak{R}}_{22} - \mathscr{P}\mathcal{I}_{12} - \mathscr{P}_4\aleph_{31}{}^2 = 0,$$
$$\ddot{\mathfrak{R}}_{22} + 2n\ddot{\mathcal{I}}_{12}' - \mathscr{Q}_1\mathfrak{R}_{22} = 0. \tag{10a}$$

and

$$\aleph_{31}'' - \mathcal{R}_1\aleph_{31} = 0. \tag{10b}$$

We set in equation (10*b*):

$$\aleph_{31}(t) = \alpha_{31}\cos(\omega t) + \beta_{31}\sin(\omega t),$$

and find that

$$(\omega^2 + \mathcal{R}_1)\aleph_{31}(t) = 0,$$

which has non-zero solution only when $\omega^2 = -\mathcal{R}_1 > 0$. One of such solutions is

$$\aleph_{11}(t) = \sin(\omega t), \tag{11}$$

which has been chosen in order to have initial velocity on the $\aleph$ axis, so as to obtain the motion out of the orbital plane. Also, by setting:

$$\mathcal{I}_{12} = \alpha_{11} + \alpha_{12}\cos(\omega t) + \alpha_{13}\cos(2\omega t) + \beta_{11}\sin(\omega t) + \beta_{12}\sin(2\omega t),$$
$$\mathfrak{R}_{22} = \alpha_{21}\cos(\omega t) + \alpha_{22}\cos(2\omega t) + \beta_{21}\sin(\omega t) + \beta_{22}\sin(2\omega t),$$

we find that the solution of system (10*a*) is:

$$\mathcal{I}_{12} = \alpha_{11} + \alpha_{12}\cos(2\omega t),$$
$$\mathfrak{R}_{22} = \beta_{22}\sin(2\omega t), \tag{12}$$

where

$$\alpha_{11} = \frac{-\mathscr{P}_4}{2\mathscr{P}_1\omega^2}, \quad \alpha_{12} = \frac{\mathscr{P}_4(\mathscr{Q}_1 + 4\omega^2)}{2\omega^2 p}, \quad \beta_{22} = \frac{-2n\mathscr{P}_4}{\omega p},$$

and $\omega = \sqrt{-\mathcal{R}_1}$, $p = 16\omega^4 + 4(\mathscr{P}_1 + \mathscr{Q}_1 - 4n^2)\omega^2 + \mathscr{P}_1\mathscr{Q}_1$. So, the periodic solution up to second order terms w.r.t. *e* is:

Figure 4. Comparison of the analytical three-dimensional solution (14) emanating from the collinear equilibrium point L_1 with the numerical one in the α-Centauri binary system in three different projections: (a) $(\mathcal{I}, \mathfrak{R}) = (x, \dot{y})$ plane, (b) $((\mathcal{I}, \aleph) = (x, \dot{z})$ plane and (c) $(\mathfrak{R}, \aleph) = (\dot{y}, \dot{z})$ plane.
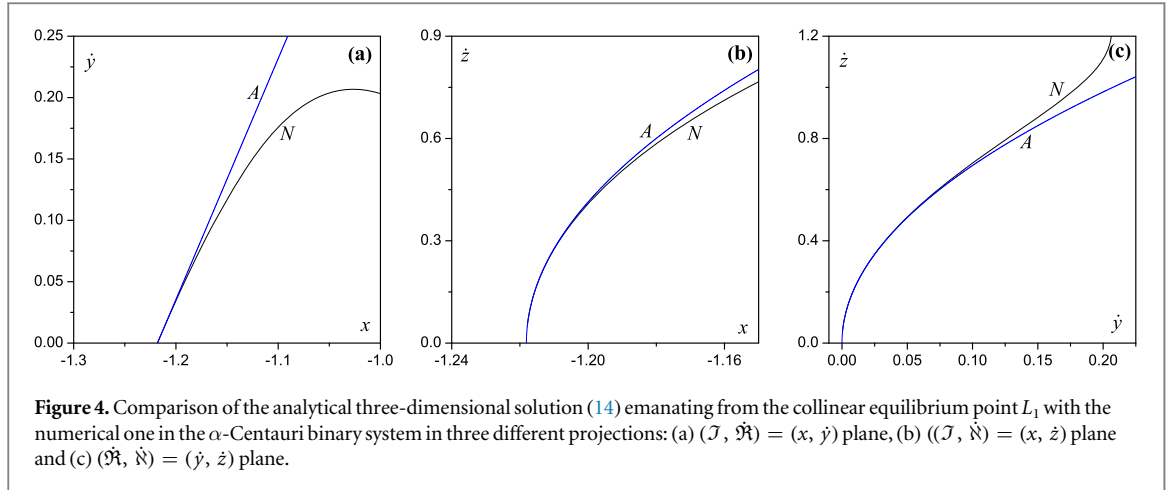
$$\mathcal{I} = x_0 + \varepsilon^2[\alpha_{11} + \alpha_{12} \cos(2\omega t)],$$
$$\mathfrak{R} = \varepsilon^2 \beta_{22} \sin(2\omega t),$$
$$\aleph = \varepsilon \sin(\omega t). \qquad (13)$$

From (13) and for $t = 0$ we obtain the initial conditions of a periodic orbit in the form:

$$(\mathcal{I}, \mathfrak{R}, \aleph, \dot{\mathcal{I}}, \dot{\mathfrak{R}}, \dot{\aleph})|_{t=0} = (x_0 + (\alpha_{11} + \alpha_{12})\varepsilon^2, \ 0, \ 0, \ 0, \ 2\omega\varepsilon^2 \beta_{22}, \ \omega\varepsilon). \qquad (14)$$

while the value of the orbital parameter ε is arbitrarily chosen.

In figure 4, we present the analytical three-dimensional solution (blue curve denoted by A) emanating from the collinear equilibrium point L_1 of the α-Centauri binary system, as this is obtained from formula (14) of our analysis and by varying the orbital parameter ε in the range of values $[0, 1.2]$. For comparison reasons and for establishing the validity of our analysis, we also give in the same plot the numerical solution of the three-dimensional periodic orbits (black curve denoted by N) emanating from the same equilibrium point as this is determined by the numerical integration of the full equations of motion (2). As we can observe from figures 4(a)–(c), our analysis is valid for small values of ε, in all the projections of the space of initial conditions $(\mathcal{I}, \mathfrak{R}, \aleph) = (x, \dot{y}, \dot{z})$.

5.2. Numerical approximation of periodic solutions

The figure eight shaped orbits occur as a result of the gravitational pull of each star of the binary system on the motion of the infinitesimal body. Since three-dimensional periodic orbits emanating from the collinear equilibrium points are of figure eight shape they are of double symmetry with respect to the Ox-axis and the Oxz plane. So, and for economy on the computations, it suffices to compute them at the quarter of their period. In particular, for the numerical determination of a three-dimensional periodic orbit of double symmetry w.r.t. the Ox-axis and the Oxz plane we integrate numerically the equations of motion with initial conditions of the form $(x_{01}, 0,0,0, x_{05}, x_{06})$, i.e. the numerical integration starts on the Ox-axis and seek a perpendicular crossing of the orbit with the Oxz plane at which obviously the condition $x_2(x_{01}, 0,0,0, x_{05}, x_{06}) = 0$ is fulfilled. Therefore, we look for the following two periodicity conditions:

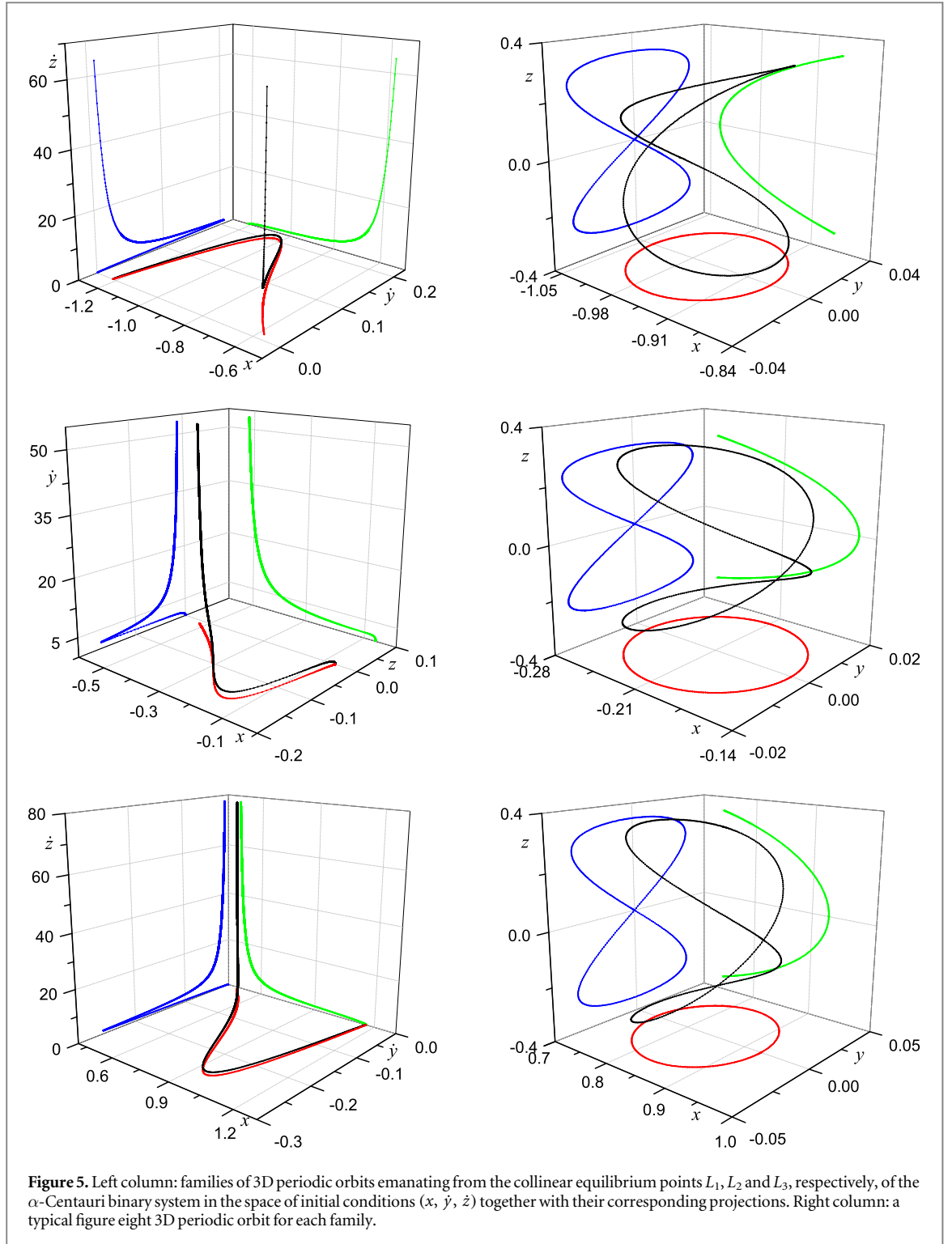$$x_4(x_{01}, 0, 0, 0, x_{05}, x_{06}) = 0, \qquad x_6(x_{01}, 0, 0, 0, x_{05}, x_{06}) = 0. \qquad (15)$$

Since two equations with three unknown components x_{01}, x_{05} and x_{06} of the initial state vector have to be satisfied we have to fix one unknown and apply well-known differential corrections procedures for the remaining two (see, e.g., Perdiou *et al* 2013). So, for choosing, e.g., $x_{06} = $ const., and by linearization of (15) we obtain the corrector system:

$$\frac{\partial x_4}{\partial x_{01}}\delta x_{01} + \frac{\partial x_3}{\partial x_{05}}\delta x_{05} = -x_4, \qquad \frac{\partial x_6}{\partial x_{01}}\delta x_{01} + \frac{\partial x_6}{\partial x_{05}}\delta x_{05} = -x_6. \qquad (16)$$

The stability of a three-dimensional periodic orbit can be determined by integrating numerically the variational equation (4). Such an orbit will be stable if simultaneously the following conditions hold (Bray and Goudas 1967, Zagouras and Markellos 1977):

$$|P| < 2 \text{ and } |Q| < 2 \qquad (17)$$

with $P = (a + \sqrt{\Delta})/2$ and $Q = (a - \sqrt{\Delta})/2$ while $\Delta = a^2 - 4(\beta - 2) > 0$ and $a = 2 - \text{Tr } V$, $\beta = (a^2 + 2 - \text{Tr } V^2)/2$, where V is the variational matrix. For stability of a three-dimensional periodic orbit in the restricted problem we also refer to Perdios (2007).

Figure 5. Left column: families of 3D periodic orbits emanating from the collinear equilibrium points L_1, L_2 and L_3, respectively, of the α-Centauri binary system in the space of initial conditions (x, $\dot{y}$, $\dot{z}$) together with their corresponding projections. Right column: a typical figure eight 3D periodic orbit for each family.

In figure 5, we present the characteristic curves, in the space of initial conditions (x, $\dot{y}$, $\dot{z}$), of the families of three-dimensional doubly symmetric periodic orbits emanating from all collinear equilibrium points of the α-Centauri binary system, as these were computed by the aforementioned procedure. In the right frames of this figure, we plot a typical figure eight member orbit for each family in the physical space while, in figure 6, where we plot the quarter of period versus the stability parameters P and Q as these were defined by (17), we give the stability diagram of the corresponding families. As we can see from this figure, stability of three-dimensional periodic orbits occurs only for families emanating from the equilibrium points L_2 and L_3 while we also observe that the period of these orbits goes to zero in the evolution of all the computed families.

This was the criterion used to stop computing them. In other words, such a member orbit with period near to zero has been considered as a termination point of any determined family. For example, the full period of the last computed three-dimensional periodic orbit of the family emanating from the collinear equilibrium point L_1
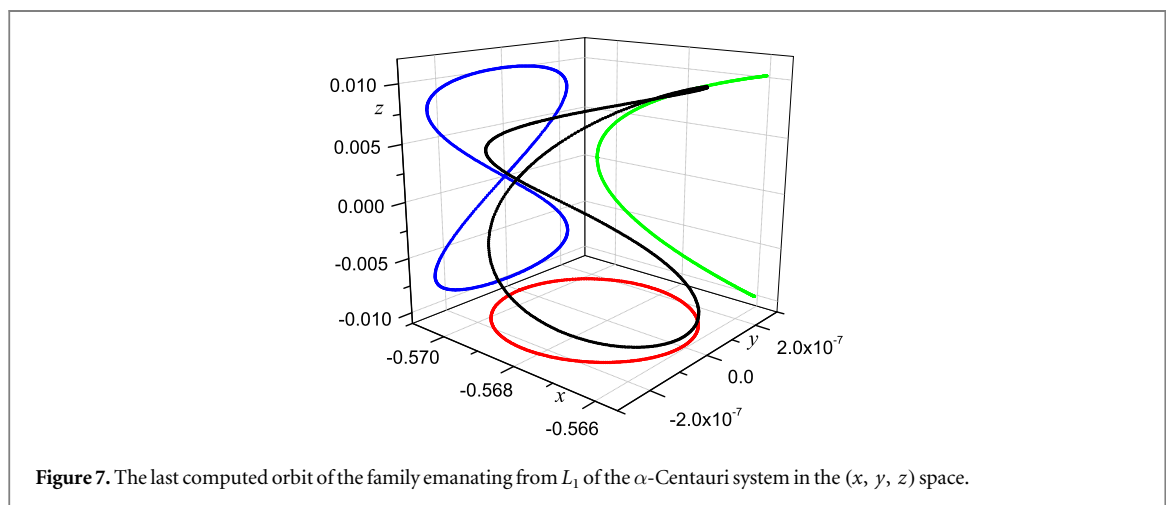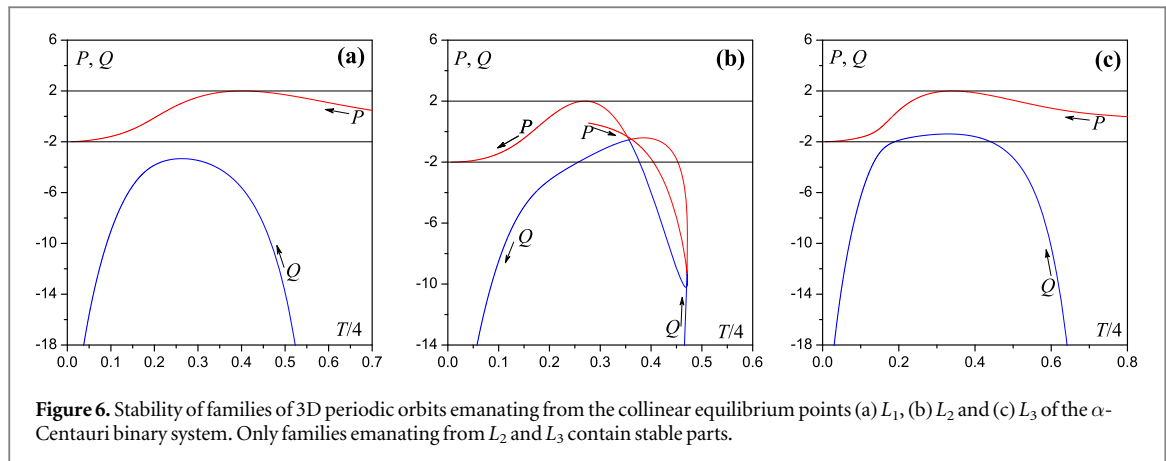
Figure 6. Stability of families of 3D periodic orbits emanating from the collinear equilibrium points (a) L_1, (b) L_2 and (c) L_3 of the α-Centauri binary system. Only families emanating from L_2 and L_3 contain stable parts.

Figure 7. The last computed orbit of the family emanating from L_1 of the α-Centauri system in the (x, y, z) space.

Table 4. Initial conditions around the collinear equilibrium point L_1.

Binary systems	x_1	$\dot{x}_2$	$\dot{x}_3$	$T/4$	C
Sirius	$-1.261\ 547\ 28$	$0.000\ 576\ 24$	0.05	$0.782\ 044\ 52$	$4.219\ 990\ 91$
Procyon	$-1.252\ 110\ 73$	$0.000\ 553\ 22$	0.05	$0.765\ 455\ 23$	$4.338\ 446\ 24$
Luhman 16	$-1.220\ 781\ 22$	$0.000\ 550\ 89$	0.05	$0.778\ 661\ 19$	$4.391\ 048\ 43$
α-Centuari	$-1.217\ 830\ 18$	$0.000\ 518\ 52$	0.05	$0.744\ 872\ 63$	$4.532\ 062\ 33$
Luyten 726-8	$-1.205\ 076\ 94$	$0.000\ 517\ 14$	0.05	$0.747\ 526\ 44$	$4.559\ 834\ 83$

of α-Centauri binary system is approximately $T \cong 0.0005$ at the value of the Jacobi constant $C \cong -3159.7$, with initial conditions $x_0 = -0.570\ 605\ 43$, $\dot{y}_0 = 0.005\ 782\ 61$ and $\dot{z}_0 = 137.629\ 642$. This member orbit is presented in figure 7 where we observe that it almost appears to exist on the Oxz plane since the values of the y coordinate are near zero.

In tables 4–6, we give initial conditions for all families of three-dimensional periodic orbits about the collinear equilibrium points of all five considered binary systems. In particular, we give the values of the orbit on the Ox-axis, i.e. $x = x_1$, $\dot{y} = x_5 = \dot{x}_2$, $\dot{z} = x_6 = \dot{x}_3$, the period up to its vertical intersection with the Oxz plane, i.e. at the quarter of the full period, as well as the value of the Jacobi constant C. We refer here to the work by Tsirogiannis *et al* (2006) where they have presented results for three-dimensional periodic orbits around the collinear equilibrium points of the restricted three-body problem in the case when the larger primary is a source of radiation and the smaller one is an oblate spheroid.

6. Conclusions

In this investigation, the primary and secondary bodies of the restricted three-body problem have been taken as oblate spheroids and radiation sources. The theory has been applied to five binary systems: Sirius, Procyon,

Table 5. Initial conditions around the collinear equilibrium point L_2.

Binary systems	x_1	$\dot{x}_2$	$\dot{x}_3$	$T/4$	C
Sirius	−0.219 729 09	−0.000 029 26	0.05	0.333 231 58	4.699 168 71
Procyon	−0.181 021 14	−0.000 021 32	0.05	0.311 879 10	4.917 128 21
Luhman 16	−0.078 613 90	−0.000 008 23	0.05	0.293 027 07	5.146 426 16
α-*Centuari*	−0.064 321 77	−0.000 005 96	0.05	0.276 767 24	5.330 841 13
Luyten 726-8	−0.026 097 26	−0.000 002 23	0.05	0.270 051 06	5.434 284 86

Table 6. Initial conditions around the collinear equilibrium point L_3.

Binary systems	x_1	$\dot{x}_2$	$\dot{x}_3$	$T/4$	C
Sirius	1.108 101 62	−0.000 731 62	0.05	0.996 044 58	3.810 796 90
Procyon	1.123 013 26	−0.000 677 16	0.05	0.935 990 28	3.979 451 14
Luhman 16	1.160 473 98	−0.000 607 77	0.05	0.853 889 76	4.215 152 29
α-*Centuari*	1.161 013 64	−0.000 572 39	0.05	0.810 357 04	4.355 100 76
Luyten 726-8	1.175 319 62	−0.000 547 79	0.05	0.780 173 18	4.462 834 31

Luhman 16, α-Centuari and Luyten 726-8. The physical parameters of each binary system were obtained and used to calculate their respective mass parameters and mass reduction factors. The number and positions of the collinear equilibrium points of each binary system were obtained numerically by combining the topological degree theory and the numerical determination of roots of nonlinear algebraic equations. The effect of the respective oblateness and radiation coefficients on the collinear equilibrium points of the binary Sirius system were shown graphically. The linear stability of the collinear equilibrium points of the five binary systems was also examined and found to be unstable in the Lyapunov sense just like in the classical case.

An analytical approximation of three-dimensional periodic motion around the collinear points was obtained by utilizing the Lindstedt–Poincaré method. The analytical solution was used in order to find suitable starting points for the numerical computation of the respective families of three-dimensional periodic orbits about the collinear points. The stability of the obtained periodic orbits for the binary α-Centuari system was also examined. Our results showed that only families emanating from L_2 and L_3 contain stable parts. Finally, we found that all the computed families, in their evolution comprised by member orbits which have decreasing period. Our termination criterion for their continuation was that the value of the full period of an orbit will be less than the value 0.0005. Using this criterion none of the determined families terminates at the physical plane which is not the usual termination of this kind of families in the restricted problem where they all go to a bifurcation with a coplanar periodic orbit, such as in the study by Tsirogiannis *et al* (2006) and Singh *et al* (2016). The choice to take the primaries to be sufficiently oblate bodies seems to be the reason where we obtain the different result in the evolution of three-dimensional periodic orbits emanating from the collinear equilibrium points of the binary α-Centuari system.

Acknowledgments

ORCID iDs

Jessica Mrumun Gyegwe ⓘ https://orcid.org/0000-0002-2082-1063

References

Abouelmagd E I, Alzahrani F, Hobiny A, Guirao J L G M and Alhothuali M 2016 Periodic orbits around the collinear libration points *J. Nonlinear Sci. Appl.* **9** 1716–27

Bray T A and Goudas C L 1967 Three-dimensional periodic oscillations about L_1, L_2, and L_3 *Adv. Astron. Astrophys.* **5** 71–130

Bosanac N, Howell K C and Fischbach E 2015 Stability of orbits near large mass ratio binary systems *Celest. Mech. Dyn. Astron.* **122** 27–52

Hénon M 1965 Exploration numérique du problème restreint: II. Masses égales, stabilité des orbites périodiques *Ann. Astrophys.* **28** 992–1007

Hénon M 1973 Vertical stability of periodic orbits in the restricted problem: I. Equal masses *Astron. Astrophys.* **28** 415–26

Hou X Y and Liu L 2009 On Lyapunov families around collinear libration points *Astron. J.* **137** 4577–85

Howell K C 1984 Three-dimensional, periodic, 'halo' orbits *Celest. Mech.* **32** 53–71

Jain S, Kumar A and Bhatnagar K B 2006 Periodic orbits around the collinear liberation points in the restricted three body problem when the smaller primary is a triaxial rigid body: Sun–Earth case *Bull. Astron. Soc. India* **34** 211–23

Jiang Y 2015 Equilibrium points and periodic orbits in the vicinity of Asteroids with an application to 216 Kleopatra *Earth Moon Planets* **115** 31–4

Kalantonis V S, Perdios E A, Perdiou A E and Vrahatis M N 2001 Computing with certainty individual members of families of periodic orbits of a given period *Celest. Mech. Dyn. Astron.* **80** 81–96

Lara M and Pelàez J 2002 On the numerical continuation of periodic orbits : an intrinsic, three-dimensional, differential, predictor-corrector algorithm *Astron. Astrophys.* **389** 692–701

Liu P, Hou X, Tang J and Liu L 2014 Application of two special orbits in the orbit determination of lunar satellites *Res. Astron. Astrophys.* **14** 1307–28

Mia R and Kushvah B S 2016 Stability and Fourier-series periodic solution in the binary stellar systems *Few-Body Syst.* **57** 851–67

Nagel E and Pichardo B 2008 A simple analytical formulation for periodic orbits in binary stars *Mon. Not. R. Astron. Soc.* **384** 548–62

Perdios E A 2007 The manifolds of families of 3D periodic orbits associated to Sitnikov motions in the restricted three-body problem *Celest. Mech. Dyn. Astron.* **99** 85–104

Perdiou A E, Nikaki A A and Perdios E A 2013 Periodic motions in the spatial Chermnykh restricted three-body problem *Astrophys. Space Sci.* **345** 57–66

Picard E 1892 Sur le nombre des racines communes à plusieurs equations simultanées *J. Math. Pure Appl.* **8** 5–24

Ragos O and Zagouras C 1991 Periodic solutions around the collinear langrangian points in the photogravitational restricted three-body problem: Sun–Jupiter case *Celest. Mech. Dyn. Astron.* **50** 325–47

Richardson D L 1980 Analytic construction of periodic orbits about the collinear points *Celest. Mech. Dyn. Astron.* **22** 241–53

Singh J and Begha J M 2011 Stability of equilibrium points in the generalized perturbed restricted three-body problem *Astrophys. Space Sci.* **331** 511–9

Singh J and Ishwar B 1999 Stability of triangular points in the photographitational restricted three-body problem *Bull. Astron. Soc. India* **27** 415–24

Singh J and Umar A 2013 On 'out of plane' equilibrium points in the elliptic restricted three-body problem with radiating and oblate primaries *Astrophys. Space Sci.* **344** 13–9

Singh J, Kalantonis V S, Gyegwe J M and Perdiou A E 2016 Periodic motions around the collinear equilibrium points of the restricted three-body problem where the primary is a triaxial rigid body and secondary is an oblate spheroid *Astrophys. J. Suppl. Ser.* **277** 13

Tsirogiannis G A, Douskos C N and Perdios E A 2006 Computation of the Liapunov orbits in the photogravitational RTBP with oblateness *Astrophys. Space Sci.* **305** 389–98

Xuetang Z and Lizhong Y 1993 Photogravitational restricted three-body problem and coplanar libration points *Chin. Phys. Lett.* **10** 61–4

Zagouras C and Markellos V V 1977 Axisymmetric periodic orbits of the restricted problem in three dimensions *Astron. Astrophys.* **59** 79–89

Zotos E E 2015 Orbital dynamics in the planar Saturn–Titan system *Astrophys. Space Sci.* **358** 4